

## CASSINI NAVIGATION DURING SOLAR CONJUNCTIONS VIA REMOVAL OF SOLAR PLASMA NOISE

P. Tortora\*, L. Iess†, J.J.B. Ordi‡, J.E. Ekelund‡, D. Roth‡

The Cassini spacecraft and its ground segment are currently testing a novel radio frequency multilink technology to perform radio science experiments. During solar conjunctions, this allows the complete removal of the solar plasma noise from the Doppler observables used for navigation. This is obtained combining the carrier frequencies of three independent down-links: two of them, a X- and a Ka-band (Ka1), are coherent with a X-band up-link, while an additional Ka-band down-link (Ka2), is coherent with a Ka-band up-link. During the June-July 2002 Cassini solar conjunction, this procedure was fully tested for the first time. We show that, using the proposed multifrequency plasma calibration scheme, the standard deviation of the Doppler frequency residuals is reduced up to a factor of 200 over the uncalibrated data. This large improvement in the data quality, revealed by values of the frequency stability previously achieved only during solar oppositions, makes the navigation accuracy of deep space probes nearly independent of the solar elongation angle.

### INTRODUCTION

Current deep space navigation systems rely on X-band radio-links, used for both range and range-rate measurements. The frequency stability of these links (measured by the Allan deviation) is on the order of  $10^{-13}$  at 1000s integration time<sup>1</sup>, yielding range-rate accuracies on the order of  $1.5 \times 10^{-3}$  cm/s. Near solar oppositions, when the sun-earth-probe (SEP) angle is close to  $180^\circ$ , higher stabilities (on the order of  $2 \times 10^{-14}$ ) can be achieved, since the solar wind velocity is nearly parallel to the line-of-sight<sup>2</sup>. The lowest stabilities are obtained, for missions in the ecliptic plane, during solar conjunctions (SEP angles close to zero) which can last up to two weeks. The degradation in the attainable navigation accuracy is caused by the signal phase scintillation due to the solar plasma. Radio metric data collected when the line of sight falls within 40 solar radii from the sun are generally not used for the orbit determination process, due to the high measurement errors introduced by the solar corona, leading to long time spans during which navigation cannot rely on actual data.

\*Università di Bologna, Istituto di Ingegneria, Via Fontanelle 4, 047100 - Forlì (FC), Italy

†Università di Roma, "La Sapienza", Dipartimento di Ingegneria Aerospaziale ed Astronautica, Via Eudossiana 18, 00184, Rome, Italy

‡Jet Propulsion Laboratory, California Institute of Technology, Navigation and Mission Design Section, 4800 Oak Grove Drive Pasadena, CA 91109 - USA

More than 30 days of tracking data, across the 2000 and 2001 solar conjunctions, were removed for the orbit reconstruction of the Cassini spacecraft, currently in cruise flight to Saturn<sup>3-5</sup>. This strategy is widely accepted and proven during the cruise flight, but it is not recommended during critical mission phases, when frequent ground-commanded maneuvers are executed. An example of this is the Cassini Saturn Orbit Insertion (SOI) maneuver, scheduled on July 1<sup>st</sup> 2004, only seven days before a solar conjunction<sup>6</sup>. In order to reduce the orbit determination uncertainties, the whole maneuver would greatly benefit from using all radio metric data collected leading up to and following SOI.

The Cassini spacecraft and ground segment are currently used to test a novel multilink radio frequency (RF) system to perform radio science experiments<sup>7</sup> (RSE). The on-board configuration provides, in addition to the standard X-band up-link/X-band down-link (X/X), an exciter (KEX) which generates a Ka-band down-link signal (at 32.5 GHz), coherent with the received X-band up-link, resulting in a X/Ka link. Moreover, a Ka/Ka link is obtained using a coherent frequency translator (KaT), which transmits to the ground a Ka-band signal (at 32.5 GHz) coherent with a Ka-band up-link (at 34 GHz). The primary goals of RSE are the measurement of the solar gravitational deflection during the Solar Conjunction Experiments (SCE)<sup>8-9</sup>, and the search for low-frequency gravitational waves (due, for example, to the coalescence of massive black hole binaries) during solar oppositions<sup>10</sup>.

The multifrequency plasma calibration scheme<sup>11</sup>, originally proposed to calibrate the Doppler observables used for the estimation of the post-Newtonian parameter  $\gamma$  during the SCE, has also shown to be very effective in improving the accuracy of the orbit determination process. This has been demonstrated during the test of the Cassini ground and on-board systems, performed on May-June 2001<sup>12</sup>, and during the June-July 2002 solar conjunction<sup>13</sup>. With this method, the sky frequencies, reconstructed using data from a wideband open loop receiver (OL) in the three bands (X/X, X/Ka, Ka/Ka) are coherently combined to remove the effects of the solar plasma, the major noise source in the Doppler observable. However, the observables used by the orbit determination program (ODP)<sup>14</sup> developed at the Jet Propulsion Laboratory, are obtained from the block V receivers (BVR) which digitally lock and track the carrier in a closed loop (CL). Thus, using the OL plasma calibrated sky frequencies for the orbit determination process requires the additional computation of Doppler observables compatible with the data format required by the ODP.

The analysis of the 2001 Cassini solar conjunction data<sup>12</sup>, has shown that the use of the multifrequency plasma calibration scheme can lower the Allan deviation to values of  $2 \times 10^{-14}$ , at integration times of 1000 s, when the impact parameter is about 25 solar radii. This corresponds to a range rate accuracy of about  $3 \times 10^{-4}$  cm/s. At an impact parameter of about 6 solar radii, the Allan deviation is on the order of  $4 \times 10^{-14}$  (1000 s integration time), still well below the corresponding original uncalibrated X-band value.

For the 2002 Cassini solar conjunction a much wider data set has been analyzed<sup>13</sup>. The results show that, while the stability of the uncalibrated links degrades as the line-of-sight get closer to the Sun, the Allan deviation of the plasma calibrated frequency residuals has nearly constant values of  $1-2 \times 10^{-14}$  at integration times of 1000 s. Similar values were previously achieved only near solar oppositions.

Moreover, at the Deep Space Network (DSN) complex located at Goldstone (CA) – DSS 25, an advanced media calibration (AMC) system has been developed and implemented to perform RSE. It consists of water vapor radiometers, digital pressure sensors and microwave temperature profilers<sup>15-16</sup> providing a precise calibration of the *dry* and *wet* frequency shifts due to the Earth troposphere. The analysis of the calibration data collected during the 2002 Cassini solar conjunction has shown that the frequency stability is improved by about a factor of 3, when the AMC, rather than the standard seasonal tropospheric models, are applied to the navigation data.

The remainder of this paper is organized as follows: first a brief description of the June-July 2002 Cassini Solar Conjunction is given, pointing out the geometry of the Cassini trajectory, as seen from the Earth, and summarizing the data acquired. Then the algorithm to reconstruct the sky frequencies from wideband OL data is illustrated, and the effect of the solar corona on signal properties is described. Then, the plasma calibration scheme, used to generate the “plasma-free” observables, is described and, using a simple model of the orbital dynamics, the stability of the obtained residuals is characterized in terms of Allan deviations and power spectra. In the next Section, the techniques for the reduction of the non-dispersive, tropospheric effects, using the advanced media calibration system, are analyzed. Finally, we show a thorough comparison among the frequency residuals and orbital solutions obtained using, in the ODP, uncalibrated and calibrated data. Concluding remarks are offered in the last Section.

## GEOMETRY OF THE 2002 CASSINI SOLAR CONJUNCTION

During June-July 2002 Cassini solar conjunction (SCE1), the radio science equipment on-board the spacecraft and at the DSN ground stations was operated to acquire the down-link signals with 24 hour coverage. At the DSS 25 complex, the only one with Ka-band uplink capability, the OL receivers acquired and sampled the down-link carrier in three bands (X/X, X/Ka and Ka/Ka), while at the DSS 45 (Cambera, Australia) and DSS 65 (Madrid, Spain) the OL receivers acquired only the X/X signal. Table 1 shows a summary of both the expected and actually acquired data for the days of year (DOY) 157/2002 to 186/2002. The geometry of the X/Ka link at DSS 25 is identical to that of the X/X link.

**Table 1: Summary of OL data acquired at DSN stations during 2002 Cassini solar conjunction**

<b>Band</b>	<b>DSN station</b>	<b>Cumulative Expected Pass Duration (hh.mm)</b>	<b>Cumulative Actual Pass Duration (hh.mm)</b>	<b>% Acquired</b>
X/X	DSS25	359.00	340.08	95%
Ka/Ka	DSS25	262.40	188.15	72%
X/X	DSS45	129.20	125.08	97%
X/X	DSS65	254.36	241.21	95%

The relatively low percentage of Ka/Ka data acquired at DSS-25 is due to a malfunctioning of the Ka-band up-link transmitter, caused by a heat exchanger problem. This resulted in either the complete absence of data for some passes or some tracks being shorter than expected.

Since the plasma calibration is made possible by the simultaneous acquisition of the down-link signals in the three bands, Table 2 summarizes the amount of multifrequency data expected and actually acquired at DSS 25; in practice it represents the intersection between the X/X and Ka/Ka data sets (rows 1 and 2 in Table 1). In Table 2, actual tracks shorter than 5 hrs have not been considered and DOY 172 has been discarded due to the high solar plasma noise.

**Table 2: Summary of multifrequency OL data acquired at DSS 25 during 2002 Cassini solar conjunction**

<b>Cumulative Expected Pass Duration (hh.mm)</b>	<b>Cumulative Actual Pass Duration (hh.mm)</b>	<b>% Acquired</b>
262.40	166.35	63%

The geometry of the 2002 Cassini solar conjunction and the relative distance of the line-of-sight vector from the center of the Sun (impact parameter), for the multifrequency data acquired at DSS 25, are shown respectively in Figures 1 and 2. The minimum SEP angle was reached on DOY 172/2002 (June 21<sup>st</sup>) at about 1:14 pm UTC, when the impact parameter was 1.6 solar radii. The multifrequency link data closest to conjunction were acquired on DOY 173/2002, at an impact parameter of about 3.5 solar radii.

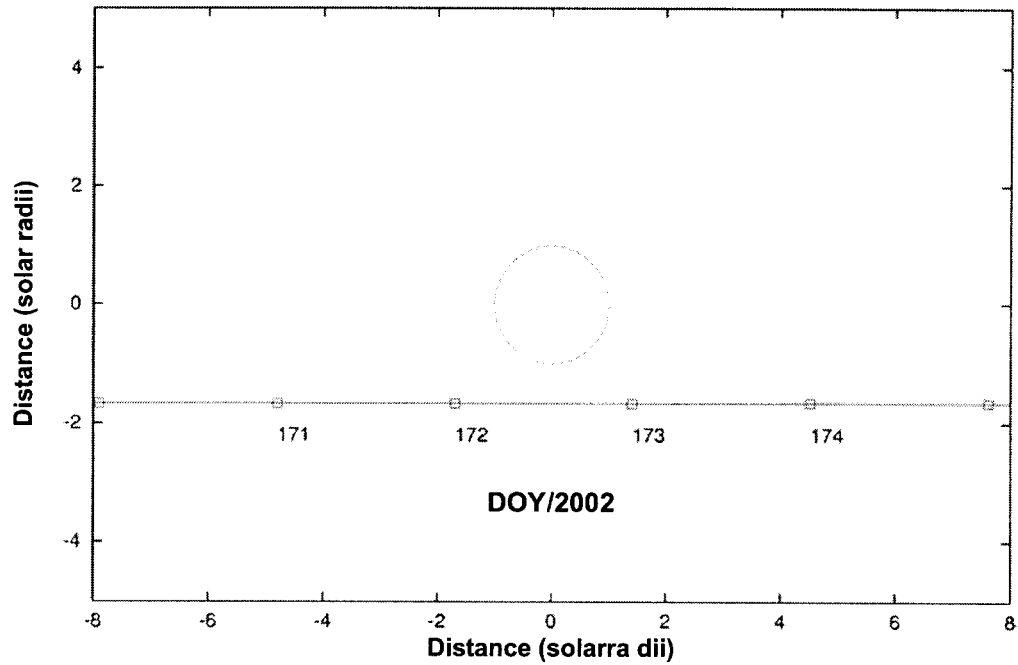


**Figure 1: Cassini trajectory with respect to the Sun  
(June-July 2002 Cassini Solar Conjunction)**

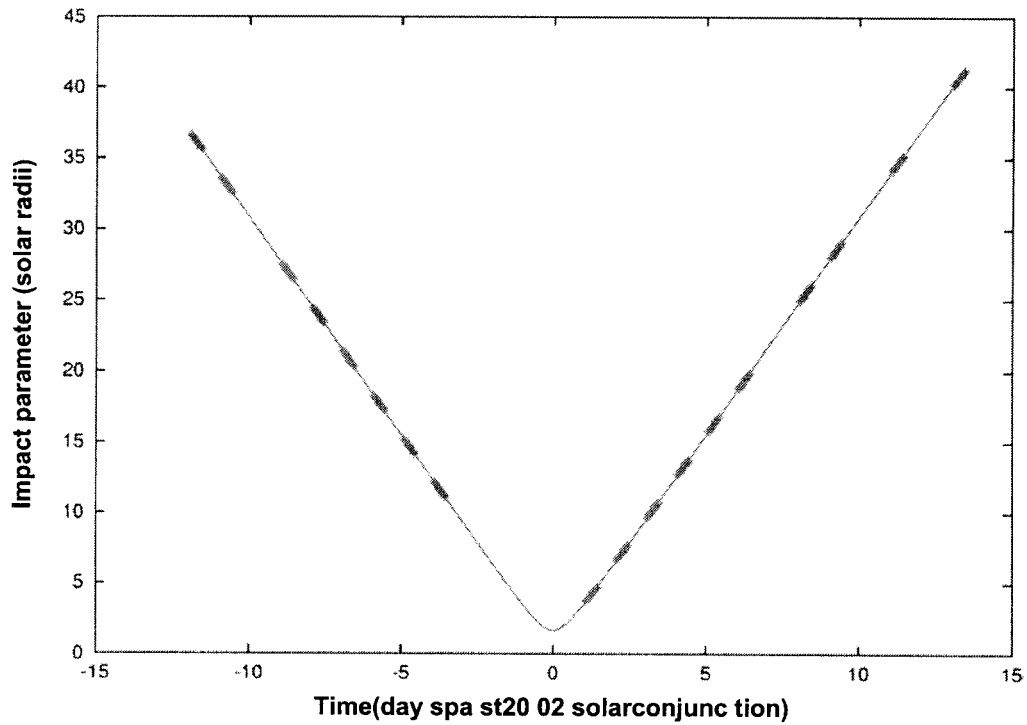


**Figure 2: Cassini impact parameter versus time  
(The data represent the time when DSS25 multifrequency tracking is available)**

## RECONSTRUCTION AND CHARACTERIZATION OF THE OPEN LOOP SKY FREQUENCIES

The radio science receiver (RSR) files, acquired at station DSS 25, consist of records of the in-phase and quadrature components of the down-converted carrier signal, plus a header containing ancillary information needed for a full reconstruction of the signal.

During conjunctions, the radio waves received at the ground station are corrupted by the solar plasma. This noise is inherently non-stationary and its effects are strongly correlated among the three bands. As the refractive index of the plasma differs from unity by a quantity proportional to the inverse square of the carrier frequency, Ka-band signals are much less affected by the corona than X-band signals. However, even a Ka-band carrier is affected by strong scintillation when the beam is very close to the sun (less than about 5 solar radii). In the RSR, the carrier is down-converted to nearly zero frequency using an accurate model of the signal dynamics, and then sampled at the pre-selected rate (1 KHz in our case). To allow for a full reconstruction, a complex representation is used where the incoming carrier is beaten against two 90° phase-shifted reference signals.

Reconstruction of signal frequency from open loop solar conjunction data has been described in Ref. 12. It has been shown that the typical algorithms used to reconstruct the signal frequency from digital samples, involving a digital Phase Lock Loop (PLL) implemented on a computer, are not suitable at impact parameters below 6-8 solar radii. The strong phase scintillation causes frequent loss of lock, especially for the X/X and X/Ka carriers, leading to a significant loss of data. This is why a different frequency reconstruction algorithm, consisting of a frequency estimator which processes sequentially (and independently) fixed-length data intervals, has been implemented to estimate the sky frequencies during solar conjunctions.

It has been shown in Ref. 13 that the sky frequencies reconstructed from open loop data exhibit large amplitude fluctuations due to the solar corona. Moreover, Ka-band data are very sensitive to the accuracy of the antenna pointing, due to the narrow beam width. This sensitivity shows up with systematic signal amplitude variations during each pass. Near conjunction, (DOY 168 and 173) all amplitudes (but especially the X/X ones) exhibit large fluctuations due to plasma scintillation.

The X/X, X/Ka and Ka/Ka observables have also been characterized by analyzing their frequency residuals<sup>13</sup>. To this end, the sky frequencies have been fitted using a simple orbital model<sup>12</sup>, based on the assumption that the signal dynamics, over time scales of a few hours (a tracking pass), is affected only by the Earth rotation and linear drifts of the spacecraft angular coordinates (right ascension and declination) and radial velocity. It turned out that the X/Ka link is the most affected by the solar plasma, as expected, essentially because the turnaround ratio of the cross-link (3344/749 ~ 4.5) amplifies the noise accumulated during the up-link signal path. Approaching and leaving conjunction, the stability of the three links is significantly degraded. In such conditions the solar plasma noise affecting the radio metric data causes a dramatic decay in the

attainable accuracy of the orbital solution. As a matter of fact, radio data collected when the line of sight falls within 40 solar radii from the Sun are usually discarded; for the Cassini orbit reconstruction, about 30 days of tracking data were removed across the 2000 and 2001 solar conjunctions<sup>5</sup>.

## COMPUTATION OF PLASMA-FREE DOPPLER OBSERVABLES USING THE MULTIFREQUENCY LINK

The output of the sky frequency reconstruction algorithm, summarized in the previous section, is as a set of three independent observables at each time instant:

$$(f_{sky})_{X/X}^{obs}, (f_{sky})_{X/Ka}^{obs}, (f_{sky})_{Ka/Ka}^{obs} \quad (1)$$

where the subscript specifies the up-link and down-link band and the superscript identifies that they are observed quantities.

Assuming that each observed sky frequency contains three independent contributions, due respectively to the spacecraft orbital motion and to the crossing of the solar corona in the up-link and in the down-link, we can define the asymptotic frequency shift and write the following equation<sup>11</sup>:

$$\begin{aligned} y_{X/X}^{obs} &= y_{nd} + y_{pl\_up} + \frac{1}{\alpha_{X/X}^2} y_{pl\_dn} \\ y_{X/Ka}^{obs} &= y_{nd} + y_{pl\_up} + \frac{1}{\alpha_{X/Ka}^2} y_{pl\_dn} \\ y_{Ka/Ka}^{obs} &= y_{nd} + \frac{1}{\beta^2} y_{pl\_up} + \frac{1}{\alpha_{Ka/Ka}^2} y_{pl\_dn} \end{aligned} \quad (2)$$

The observable frequency shifts have been computed from the observed sky frequencies as:

$$\begin{aligned} y_{X/X}^{obs} &= \frac{(f_{sky})_{X/X}^{obs}}{\alpha_{X/X} (f_X)_\uparrow} - 1 \\ y_{X/Ka}^{obs} &= \frac{(f_{sky})_{X/Ka}^{obs}}{\alpha_{X/Ka} (f_X)_\uparrow} - 1 \\ y_{Ka/Ka}^{obs} &= \frac{(f_{sky})_{Ka/Ka}^{obs}}{\alpha_{Ka/Ka} (f_{Ka})_\uparrow} - 1 \end{aligned} \quad (3)$$

where  $\alpha_{X/X} = 880/749$ ,  $\alpha_{X/Ka} = 3344/749$  and  $\alpha_{Ka/Ka} = 14/15$  are the turnaround ratios for the three links and  $\beta = (f_{Ka})_\uparrow / (f_X)_\uparrow$  is the ratio between the X and Ka-band up-link frequencies. In Eq. (2),  $y_{nd}$  is the orbital (*non dispersive*) contribution, while  $y_{pl\_up}$  and

$y_{pl\_dn}$  are respectively the *plasma up-link* and *plasma down-link* contributions to the relative frequency shift (referred to a  $(f_X)_\uparrow$  carrier).

The set of equations (2) is easily solved for  $y_{nd}$ ,  $y_{pl\_up}$ , and  $y_{pl\_dn}$ :

$$y_{pl\_dn} = \left( \frac{1}{\alpha_{X/X}^2} - \frac{1}{\alpha_{X/Ka}^2} \right)^{-1} (y_{X/X}^{obs} - y_{X/Ka}^{obs}) \quad (4)$$

$$y_{pl\_up} = \frac{y_{X/Ka}^{obs} - y_{Ka/Ka}^{obs} - y_{pl\_dn} \left( \frac{1}{\alpha_{X/Ka}^2} - \frac{1}{\beta^2} - \frac{1}{\alpha_{Ka/Ka}^2} \right)}{1 - \frac{1}{\beta^2}} \quad (5)$$

$$y_{nd} = y_{Ka/Ka}^{obs} - \left( y_{pl\_up} + \frac{1}{\alpha_{Ka/Ka}^2} y_{pl\_dn} \right) \frac{1}{\beta^2} \quad (6)$$

Once solved for the non-dispersive relative frequency shift  $y_{nd}$ , one can compute the *non dispersive sky* frequency for each band. So, for example, the non dispersive sky frequency for the X/X band can be written as:

$$(f_{sky})_{X/X}^{nd} = (f_{sky})_{X/X}^{obs} - \alpha_{X/X} (\Delta f_X)^{pl\_up} - \frac{(\Delta f_X)^{pl\_dn}}{\alpha_{X/X}} \quad (7)$$

where  $(\Delta f_X)^{pl\_up} = y_{pl\_up} (f_X)_\uparrow$  and  $(\Delta f_X)^{pl\_dn} = y_{pl\_dn} (f_X)_\uparrow$ .

Substituting in Eq.(7) and dividing by  $\alpha_{X/X} (f_X)_\uparrow$  we get:

$$\frac{(f_{sky})_{X/X}^{obs}}{\alpha_{X/X} (f_X)_\uparrow} = \frac{(f_{sky})_{X/X}^{nd}}{\alpha_{X/X} (f_X)_\uparrow} + y_{pl\_up} + \frac{y_{pl\_dn}}{\alpha_{X/X}^2}$$

which offers, by comparison with the first row of the set of equations (2), and using Eq. (3), the result:

$$(f_{sky})_{X/X}^{nd} = (1 + y_{nd}) \alpha_{X/X} (f_X)_\uparrow \quad (8)$$

Eq. (8) shows that the so-called “plasma-free” (non-dispersive) sky frequency (X/X band) is obtained as a linear combination of the three X/X, X/Ka and Ka/Ka observables since, as shown in Eq. (6), they all contribute to the non-dispersive frequency shift  $y_{nd}$ . The stability of the plasma-free link can be compared to the corresponding uncalibrated links by computing the Allan deviation of the frequency residuals obtained by fitting the sky frequency with the simple orbital model described in the previous section.

Figure 3 shows a cumulative plot of the Allan deviations (at 1000s int. time) for the available multifrequency link passes. For each pass the stability of the raw X/X, X/Ka and Ka/Ka links are directly compared to the corresponding plasma-free one. To avoid excessive contamination from tropospheric noise and systematic errors, only data acquired above 20° of elevation have been considered.

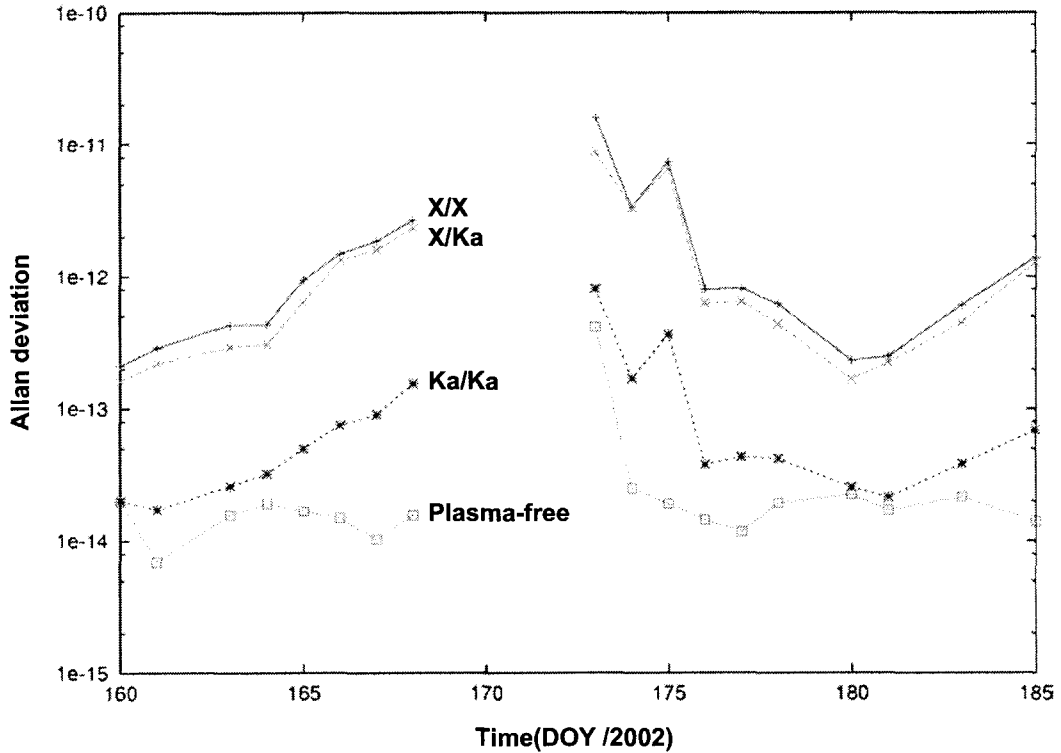


**Figure 3: Cassini 2002 solar conjunction Allan deviations @ 1 000s int. time**

While for the X/X, X/Ka and Ka/Ka links the Allan deviation degrades getting closer to the DOY 172/2002 (when the minimum SEP angle occurs) the plasma-free signal exhibits a nearly constant stability at levels of  $1-2 \times 10^{-14}$ , at integration times of 1000 s, a value previously achieved only near solar oppositions. The largest improvement in the signal stability is obtained for the DOY 175/2002, where the Allan deviation of the uncalibrated X/X signal is reduced by about 3 orders of magnitude. However, on DOY 173/2002 the plasma-free signal stability is about 50 times worse than its average value. This can be explained by considering that three main effects limit the applicability of the plasma calibration scheme (Eq. 2) based upon multi-frequency links:

- Diffraction and physical optics effects
- Magnetic corrections to the refractive index
- Spatial separation between the ray paths at different frequencies

In Ref. 12 it was thoroughly explained that at small impact parameters the diffraction effects due to physical optics are responsible for the occasional signal fading at small SEP angles. Moreover, when the impact parameter is smaller than 5 solar radii (as it was on DOY 173/2002 – see Figure 2) both magnetic corrections to the refractive index and density gradients in the solar corona (which cause a change in the impact parameter) become non-negligible.

In conclusion, Figure 3 shows that for the 30 days of the SCE1, the quality of the plasma calibrated Doppler observables is nearly independent of the SEP angle, with the exception of the pass on DOY 173/2002 where the impact parameter of the signal beam was smaller than 5 solar radii.

## **THE ADVANCED MEDIACALIBRATION SYSTEM**

To perform the RSE, the DSS 25 complex has been equipped with an outstanding media calibration system<sup>15-16</sup> capable of providing a full calibration of the dry and wet path delays due to the Earth troposphere. It consists of two independent systems, where water vapor radiometers, digital pressure sensors and microwave temperature profilers have been installed and symmetrically located a short distance from the main 34m antenna at the Goldstone complex. This system was tested for the first time during the first gravitational wave experiment (GWE1), on November 2001-January 2002<sup>10</sup>.

In Ref. 9, the data reduction of the AMC acquired during the SCE1 has been described in detail. By comparison with the corresponding data acquired during the GWE1, it has been shown that for many passes, the dry component of the zenith path delay was much noisier than expected. It turned out that the larger zenith path delay fluctuations levels were, with high probability, due to the surface wind speed which, during many passes of the SCE1, exceeded the 15-20 mph. The increased zenith path delay “noise” levels then, should be due to the atmosphere and not some wind-induced “jiggle” in the pressure sensor mechanism. This can be seen in the substantial agreement of the zenith path delays, as read from the systems 1 and 2. An easy way to filter out the high frequency dry zenith path delay fluctuations to average, through a moving window (a 100 s interval has been used for the SCE1), the raw data acquired by the instruments, in order to remove the local, small scale effects.

The parallel analysis of the GWE1 and SCE1 advanced media calibrations data has revealed that the use of the water vapor radiometers and digital pressure sensors is more effective during solar conjunctions. This is mainly due to two concurrent reasons: first, SCE are carried out during daytime while GWE take place during the night; second, due to Cassini’s present orbital position, for the northern hemisphere ground stations, the SCE observations are made in summer while the GWE ones are in winter. As a result, the tropospheric noise levels, which can be canceled making use of the AMC, are significantly higher during SCE than GWE. As shown in the next section, the frequency stability is improved by about a factor of 3, when the AMC, rather than the standard seasonal tropospheric models, are applied to the SCE1 navigation data.

## CASSINI ORBIT DETERMINATION USING PLASMA AND TROPOSPHERE CALIBRATED NAVIGATION OBSERVABLES

In the previous sections we pointed out the procedures needed to compute a plasma free sky frequency using three independent signals simultaneously acquired in the bands X/X, X/Ka and Ka/Ka. These calibrated sky frequencies can now be used to form a plasma-free Doppler observable compatible with the data format usually handled by the ODP. For two-way Doppler observables<sup>§</sup> the ODP uses the received sky frequency in the following manner to compute the observable<sup>17</sup>:

$$obs = \alpha_{Up/Dn} \cdot f_{REF} - f_{sky} \quad (9)$$

where  $f_{REF}$  is the Doppler reference frequency and  $\alpha_{Up/Dn}$  is the turnaround ratio, which depends only upon the down-link band, since it is always referred to an S-band up-link carrier. For an X-band down-link signal,  $\alpha_{S/X} = 880/221$ . Thus, at each time tag, the plasma calibrated sky frequency can be directly substituted to the corresponding uncalibrated one to form a plasma calibrated observable:

$$(obs)_{X/X}^{nd} = \alpha_{S/X} \cdot f_{REF} - (f_{sky})_{X/X}^{nd} \quad (10)$$

The result of this procedure is a new navigation file where the Doppler observables, to be processed by the ODP, are free from solar plasma noise. This new observable has been computed using OL data (RSR files and a digital frequency estimator), which have been processed for the first time for orbit determination.

For a full comparison between the plasma-free and raw observables, we processed (in the ODP) the original, plasma free and plasma free with the AMC navigation files, where the observables are computed at 300s.

To compare the results of using the three different tracking data sets in terms of spacecraft navigation, a short arc, spanning just the solar conjunction period (between June 9<sup>th</sup> and July 5<sup>th</sup>, 2002), was processed. The initial conditions on June 9<sup>th</sup>, 2002 were obtained from a long arc solution that has an epoch of February 28<sup>th</sup>, 2001. The only parameters estimated in the short arc solutions were the spacecraft state and the radioisotope thermoelectric generator (RTG) radiation accelerations. For all three cases, only station DSS 25 two-way Doppler data were used. The weights assigned to the tracking data were assigned on a pass-by-pass basis, where the a priori uncertainty assigned to each pass is equal to the  $1-\sigma$  value of their frequency residuals.

---

<sup>§</sup> One-way, two-way and three-way Doppler observables are formed respectively when:

- the spacecraft (S/C) generates a signal which is received at the ground station
- the ground station generates the up-link signal to the S/C and receives the down-link signal from it
- the up-link signal to the S/C is generated in a ground station and the down-link signal from the S/C is received in a different ground station

Figure 4 shows the two-way Doppler frequency residuals obtained by running the ODP and using the original (uncalibrated), X-band tracking datafile.

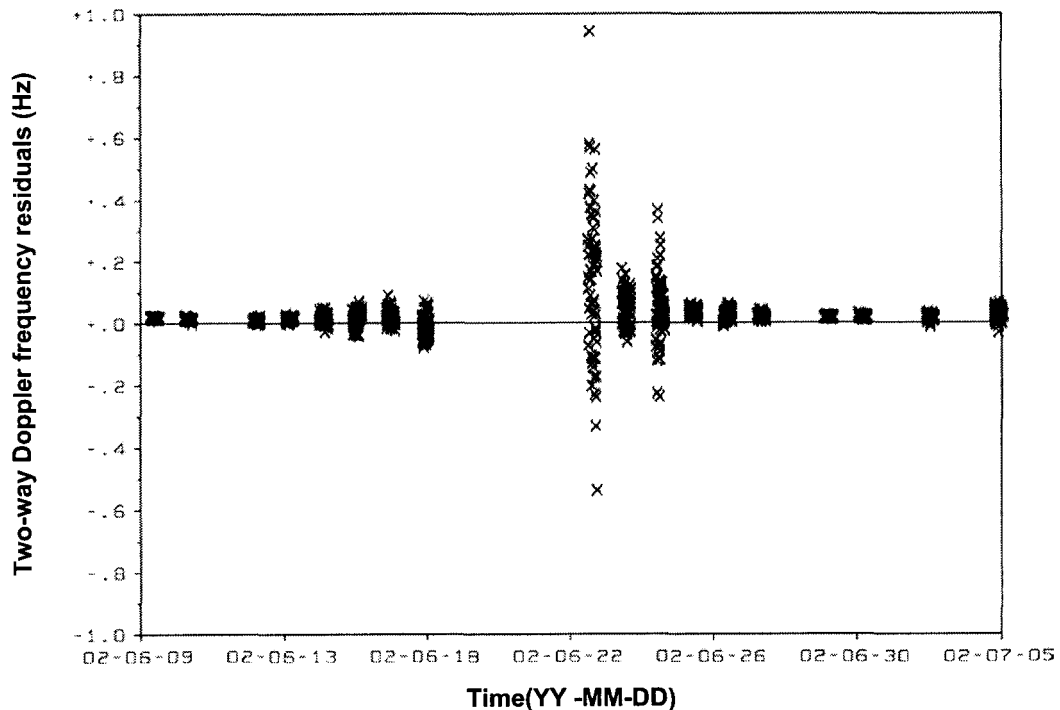


**Figure 4: Cassini 2002 solar conjunction X/X Doppler frequency residuals obtained using plasma uncalibrated data and the standard troposphere corrections**

Note the increasing variation of the frequency residuals when the spacecraft gets close to conjunction (which occurred on June 21<sup>st</sup>). On June 24<sup>th</sup>, 2002, when the average level of the residuals was already getting back to lower values, there is an evident signature in the data, already noticed in terms of increased Allan deviations in Figure 3. This was probably caused by a strong solar event in a direction perpendicular to the Earth-to-Cassini line of sight. The overall 1- $\sigma$  value of these residuals is  $7.16 \times 10^{-2}$  Hz.

Figure 5 shows exactly the same time interval of Figure 4, but now the plasma calibrated two-way Doppler observables have been processed. The y-axis scale reveals that the noise reduction is huge with nearly constant levels for the 17 passes shown. The June 22<sup>nd</sup>, 2002, pass has not been included in the plot since it is the only one where the multifrequency plasma calibration scheme did not offer reliable results – see Figure 3. The 1- $\sigma$  value of the plasma calibrated frequency residuals is  $3.5 \times 10^{-4}$  Hz, more than 20 times better than the corresponding uncalibrated ones.

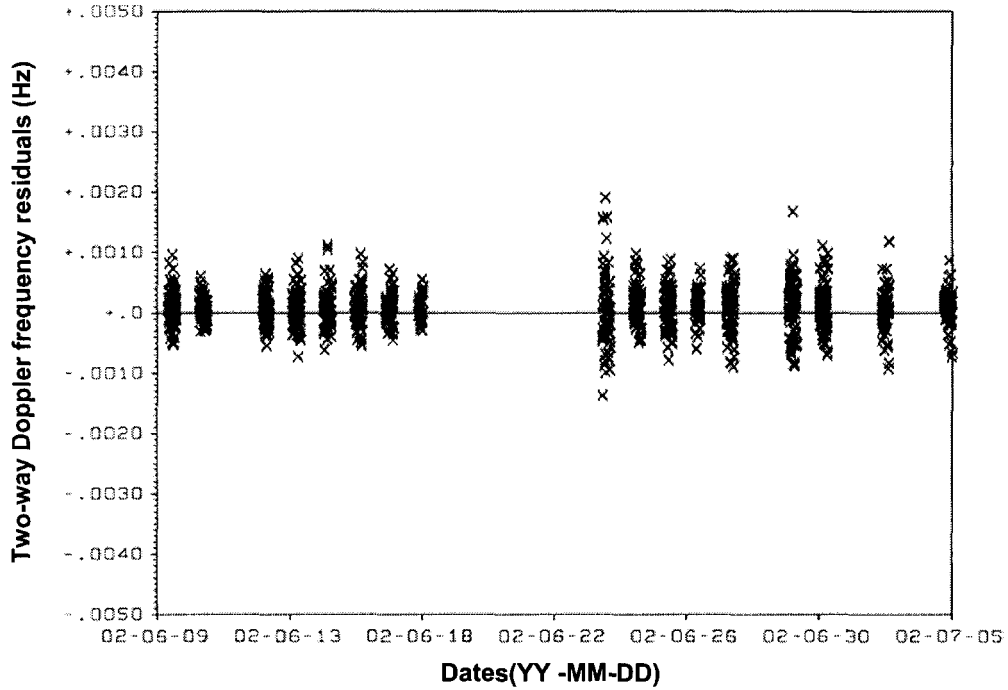


**Figure 5: Cassini 2002 solar conjunction X/X Doppler frequency residuals obtained using plasmacalib ratedata and the standard troposphere corrections**

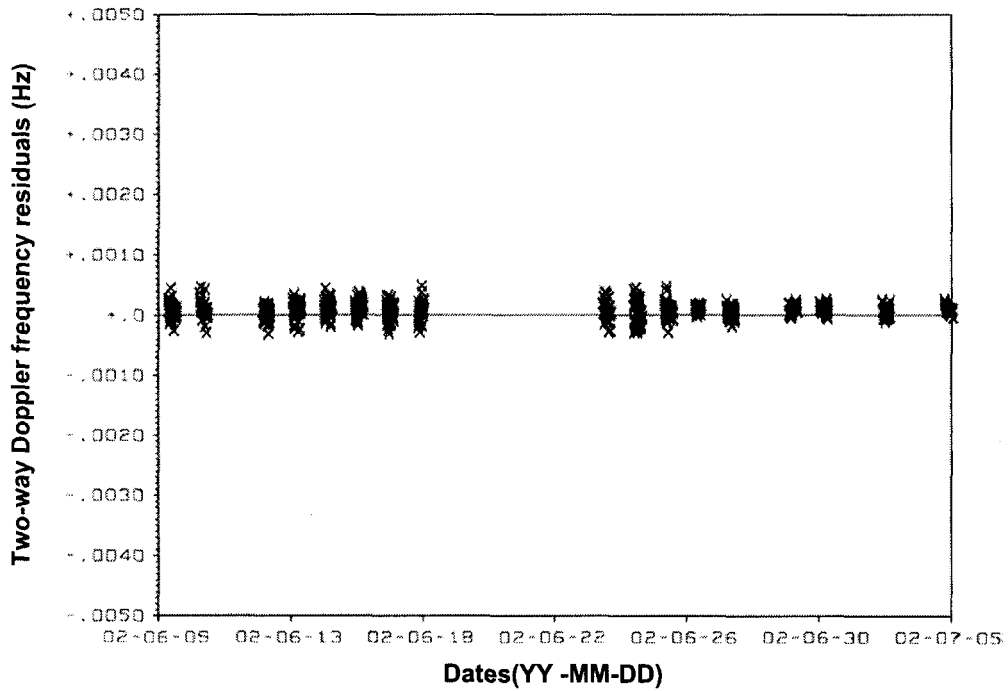


**Figure 6: Cassini 2002 solar conjunction X/X Doppler frequency residuals obtained using plasmacalib ratedata and the advanced mediacalib rations**

Figure 6 shows the additional improvement in the stability of the frequency residuals, which can be obtained once the AMC are applied to the plasma calibrated navigation observables. For some passes, especially after conjunction, the noise reduction is close to a factor of 5, while for some others the effectiveness of the advanced troposphere calibration is less evident. The  $1\text{-}\sigma$  value of the plasma calibrated frequency residuals is  $1.2 \times 10^{-4}$  Hz, respectively a factor of 3 and 600 better than the corresponding plasma calibrated and uncalibrated ones.

In order to help visualize the differences in the solutions and their uncertainties in the estimates, the results are mapped forward to the Saturn B-plane in Figure 7. For reference, the long arc solution and error ellipse is also shown in this figure. The long arc solution is considered the best estimate as of July 2002 of the Saturn B-plane location, so it provides a measure of the accuracy of the short arc solutions. The uncalibrated solution is clearly the poorest, with a large offset in the B.T direction relative to the long arc solution. The solution made with the plasma calibrated data shows a significant improvement in the level of agreement with the long arc solution. Furthermore, the addition of the advanced media calibrations results in even better agreement with the long arc solution.

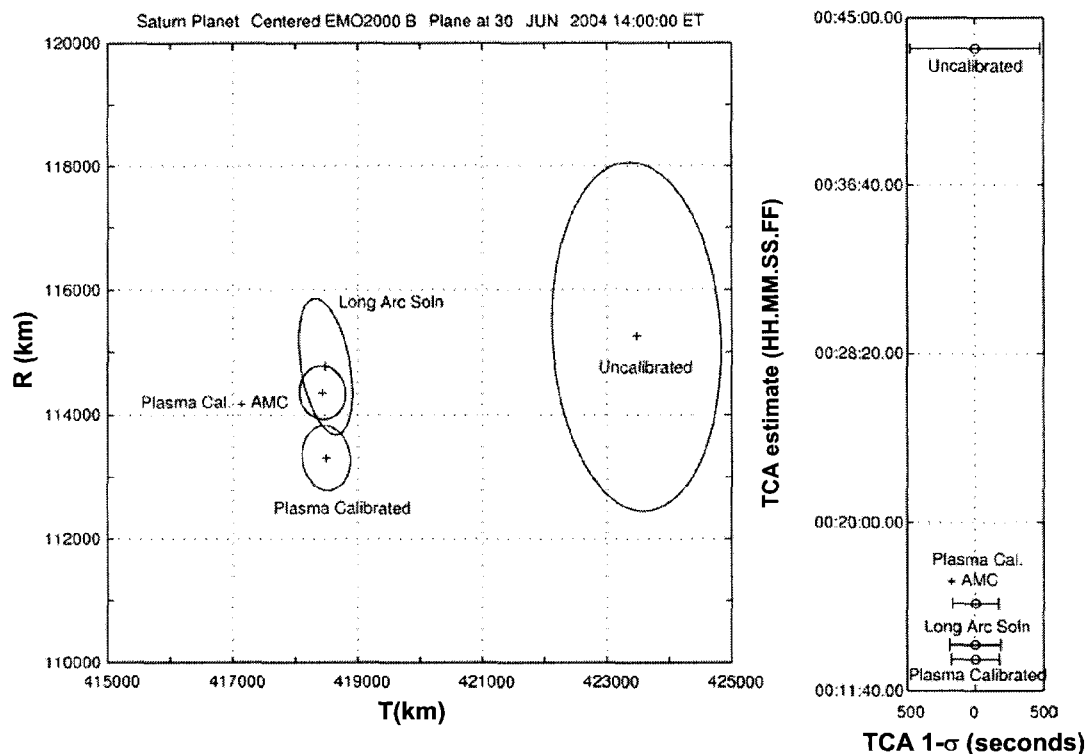


**Figure 7: Saturn centered B-plane plot of the Cassini orbital solutions obtained using different sets of X-band data collected during the 2002 solar conjunction. On the right the different estimates of the time of closest approach**

These results are impressive when considering that the short arc solutions rely on roughly 30 days of Doppler data from only one ground station during solar conjunction. It should be pointed out that these error ellipses and associated mean values in this plot are for comparison purpose only and do not represent current best knowledge of Cassini's ephemeris. In all cases, no attempt was made to model the errors associated with future maneuvers or thrusting events, which would normally dominate the size of the error ellipse. Furthermore, the actual mean values will differ because future spacecraft maneuvers and orientation changes (that will impact the direction of the radiation accelerations) are not modeled.

Another way to assess the quality of the solutions is to compare the value of the RTG acceleration estimate in the spacecraft z-direction. A very accurate estimate of this value was made during the GWE1. The RTG acceleration estimate is very precise since during the GWE1 the spacecraft orientation was not changed and was maintained using the reaction wheels rather than the reaction control thrusters. Additionally, continuous 24 hour tracking of the spacecraft was available during the GWE. The z-direction of the RTG acceleration was well determined since the spacecraft was oriented such that the z-axis was pointed towards Earth. Table 3 shows the values of the estimates of this parameter for the three different short arc cases, as well as the estimate from the long arc solution. Once again, the results show a dramatic improvement in comparison to the long arc solution when the solar plasma calibrations are included in the Doppler data. However, little improvement is seen in this parameter when the advanced media calibrations are included in the tracking data.

**Table 3: Summary of the RTG acceleration estimates obtained using different sets of X-band data and ODPs**

Case	RTG acceleration Km/s <sup>2</sup>	1 $\sigma$ uncertainty Km/s <sup>2</sup>
Long Arc Solution	-2.98 $\times 10^{-12}$	0.05 $\times 10^{-12}$
Uncalibrated Short Arc	-7.44 $\times 10^{-12}$	1.12 $\times 10^{-12}$
Plasma Calibrated Short Arc	-2.89 $\times 10^{-12}$	0.13 $\times 10^{-12}$
Plasma Calibrated + AMCS Short Arc	-3.07 $\times 10^{-12}$	0.08 $\times 10^{-12}$

## CONCLUSIONS

The Cassini spacecraft and its ground segment are equipped with an advanced radio frequency system (RF) to perform radio science experiments. In addition to the standard X-band down-link, coherent with a X-band up-link, the spacecraft on board configuration allows two additional down-links in the Ka-band, one coherent with the X-band up-link and the other coherent with a Ka-band up-link. The simultaneous acquisition of the three down-link carriers is possible only at the Goldstone (CA) complex – DSS 25 – which is the only DSN station with a Ka-band up-link and down-link capability. This configuration, originally devised to perform an accurate test of the general relativity during solar conjunctions, allows the complete removal of the solar plasma noise from the Doppler observables. Moreover, the DSS 25 has been equipped with an advanced media calibration system which allows the full calibration of the dry and wet path delay components of the Earth's troposphere.

During the 2002 Cassini solar conjunction experiment, the RF system was operated continuously for 30 days, from June 6<sup>th</sup> through July 5<sup>th</sup>. The multifrequency plasma calibration scheme has been applied to all those DSS 25 passes where the three independent down-links were available (18 passes in total). Then, the plasma-free Doppler observables, derived from radio science open loop receivers, have been fitted using the orbit determination program (ODP) to test the capabilities of the new system for precision spacecraft navigation. In addition, the advanced troposphere calibrations have been applied to the plasma calibrated data resulting in a data set of the highest quality. The analysis of the ODP frequency residuals reveals that the application of the plasma and troposphere calibrations to the Doppler observables yields a global improvement of a factor of 600 over the corresponding uncalibrated data. Thus, with this new technique, the data acquired near solar conjunctions can be successfully calibrated in order to gain frequency stabilities and orbital solution accuracies usually recorded when the spacecraft is at solar oppositions.

During the 2003 Cassini solar conjunction experiment (SCE2), a real time test of the plasma calibration technique proposed in this paper will be performed. The 30 days of continuous multifrequency tracking from DSS 25 will have the main goal of a second precise test of General Relativity, but will also allow to gain further confidence in the capabilities of this novel method for spacecraft navigation. This experience is valuable in view of the potential applications for the Saturn orbit insertion maneuver (SOI) (which occurs only 7 days before a solar conjunction, on July 1<sup>st</sup>, 2004) and during the four solar conjunctions which will occur during the Cassini Saturn tour (2004-2008).

## ACKNOWLEDGMENTS

The work of P.T. and L.I. has been funded by the Italian Space Agency (ASI). The work of J.J.B., J.E.E. and D.R. was performed at the Jet Propulsion Laboratory, California Institute of Technology, under a contract with the National Aeronautics and Space Administration.

## REFERENCES

1. Thornton, C.L., Border, J.S., "Radiometric Tracking Techniques for Deep-Space Navigation", *Deep-Space Communication and Navigation Series*, JPL Publication 00-11, Oct. 2000.
2. Armstrong, J.W., Woo, R., Estabrook, F.B., "Interplanetary Phase Scintillation and the Search for Very Low Frequency Gravitational Radiation", *The Astrophysical Journal*, Vol. 230, 1979, pp. 570-574.
3. Roth, D.C., Guman, M.D., Ionasescu, R., Taylor, A.H., "Cassini Orbit Determination From Launch to the First Venus Flyby", *Paper AIAA 98-4563, AIAA/AAS Astrodynamics Specialist Conference*, August 10-12 1998, Boston, MA, USA.
4. Guman, M.D., Roth, D.C., Ionasescu, R., Goodson, T.D., Taylor, A.H., Jones, J.B., "Cassini Orbit Determination From First Venus Flyby to Earth Flyby", *Advances in the Astronautical Sciences, Spaceflight Mechanics 2000*, Vol. 105, pp. 1053-1072.
5. Roth, D.C., Guman, M.D., Ionasescu, R., "Cassini Orbit Reconstruction From Earth To Jupiter", *Advances in the Astronautical Sciences, Spaceflight Mechanics 2002*, Vol. 112, pp. 693-704.
6. Cassini Mission Plan, Rev. N, JPL D-5564, May 2002.
7. Kliore, A.J., et al. "Cassini Radio Science", *Accepted for publication on Space Science Reviews*.
8. Iess, L., Giampieri, G., Anderson, J.D., Bertotti, B., "Doppler measurement of the solar gravitational deflection", *Classical and Quantum Gravity*, Vol. 16, 1999, pp. 1487-1502.
9. Iess, L. et al., "The Cassini Solar Conjunction Experiment: a New Test for General Relativity", *Proceeding of the IEEE Aerospace Conference*, March 8-15, 2003, Big Sky, Montana, USA.
10. Abbate, S.F., et al. "The Cassini Gravitational Waves Experiment", *Proceedings of the SPIE Conference 4856 on "Astronomy Outside the EM Spectrum"*, August 2002, Waikoloa, HI, USA.
11. Bertotti, B., Comoretto, G., Iess, L., "Doppler Tracking of Spacecraft with Multifrequency Links", *Astronomy & Astrophysics*, Vol. 269, 1993, pp. 608-616.
12. Tortora, P., Iess, L., Ekelund, J.E., "Accurate Navigation of Deep Space Probes using Multifrequency Links: the Cassini Breakthrough during Solar Conjunction Experiments", *Proceedings of The World Space Congress*, October 10-19, 2002, Houston, USA.
13. Tortora, P., Iess, L., Herrera, R.G., "The Cassini Multifrequency Link Performance during 2002 Solar Conjunction", *Proceedings of the IEEE Aerospace Conference*, March 8-15, 2003, Big Sky, Montana, USA.
14. Ekelund, J.E. et al., "Orbit Determination Program (ODP) Reference Manual", JPL D-18671 (JPL internal document), Volume 1-4, Pasadena, CA, Feb. 2000.
15. Resch, G. M. et al. "The Media Calibration System for Cassini Radio Science: Part III", *IPN Progress Report*, 42-148, 1-12, 2002.
16. Keihm, S. J., "Water Vapor Radiometer Measurements of the Tropospheric Delay Fluctuations at Goldstone over a Full Year", *TDA Progress Report*, 42-122, 1-11, 1995.
17. Moyer, T.D., "Formulation for Observed and Computed Values of Deep Space Network Data Types for Navigation", *Deep-Space Communications and Navigation Series*, JPL Publication 00-7, Oct. 2000.